ISSN 1870-4069

Corneal Topography Using a Null-screen Target in a Quadrangular Prism Configuration

M. I. Rodríguez-Rodríguez[1,*], A. Abril Suarez-Ajoleza[1],
D. Aguirre-Aguirre[2], D. González-Utrera[2],
R. Díaz-Uribe[2], A. Carmichael Martins[3], Brian Vohnsen[4]

[1] Facultad de Estudios Superiores Iztacala UNAM,
Mexico

[2] Instituto de Ciencias Aplicadas y Tecnología,
Universidad Nacional Autónoma de México,
Mexico

[3] Indiana University School of Optometry, Bloomington,
Ireland

[4]Advanced Optical Imaging Group, School of Physics,
University College Dublin,
Ireland

martin.isaias.rodriguez@iztacala.unam.mx

Abstract. In previous works, three reflective calibration spheres of different radius of curvature (7.7 mm, 9.42 mm, and 6.20 mm) were evaluated using an experimental setup based on specular reflection. To build this system; we use four identical null-screens into a quadrangular acrylic prism. The aim of this work is to show that the same setup is suitable as a corneal topographer instead of the traditional commercial topographers based in Placido disk. To achieve this purpose, experimental images of a volunteer´s cornea were obtained from the reflection of an adaptable Hartmann-pattern. With the experimental parameters of the elements involved in the setup and the spot centroid data obtained by image processing, the local normals of the surface at sampled points were found. Accurate reconstruction of the surface shape of a human cornea is obtained by numerical integration of the normals. By fitting the recovered data to a spherical model the corresponding elevation map and radius of curvature 7.84 mm were found. This is the first report of the evaluation of a corneal surface using a null-screen target in a quadrangular prism configuration.

Keywords: Null-Screens, Hartmann pattern, numeric integration method, corneal topography.

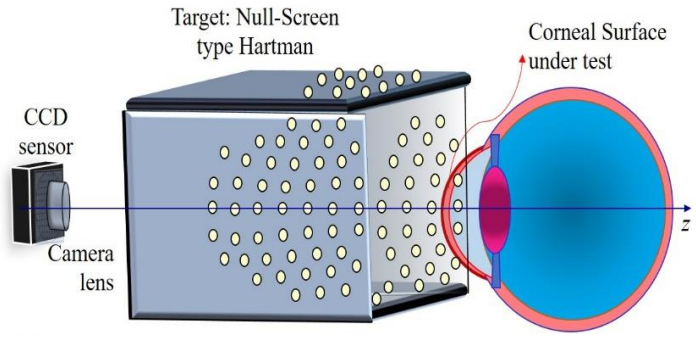

Fig. 1. Schematic setup of a quadrangular prism configuration [10].

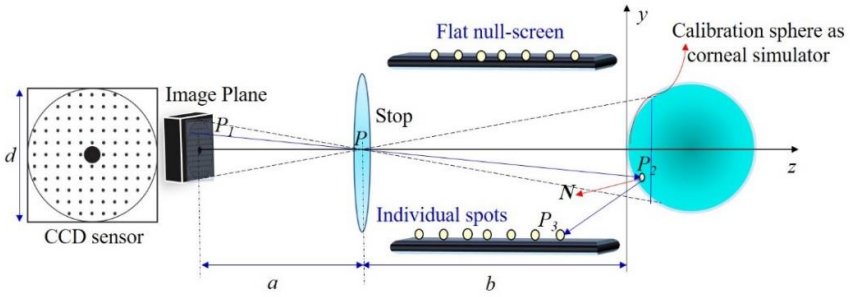

Fig. 2. Variables involved in the calculation of flat null-screen.

1. Introduction

It is well known that the anterior corneal surface provides about three-quarters parts of the total dioptric power of the human eye. On the other hand, refractive corrections and monitoring of corneal ectasias and keratoconus are all measured by corneal topography. Thus, quantifying corneal parameters such as radius of curvature, refractive power and elevation maps are of great research value and essential for vision and diagnostics. The studies about corneal topography have typically made use of a Placido disc or Scheimpflug ophthalmology [1]. However, a possible limitation of Placido system due to data ambiguity in azimuthal direction was reported in 1998 by Schwiegerling et al. [2], what's more; "Axial curvature and the skew ray error in corneal topography" was reported in 1997 by S.A. Klein [3-4]. Consequently, new generations of topographers were developed making use of different principles with a geometrical pattern of spots printed on null-screens and in a modified Hartmann test to measure corneal topography [5-7]. These recent advances have been successful in testing, because modifying the geometry it can overcome the skew ray error.

The null-screen method has been used to test different types of optical surfaces as; spherical, aspherical fast convex and recently freeform surfaces [5-9]. For this reason,

we have been working on a method for testing the corneal surface with four flat null-screens in a quadrangular prism setup, based on the null-screen principles. In a previous work, we have demonstrated quantitatively that three reflective calibration spheres of different radius of curvature; 7.7 mm, 9.42 mm, and 6.20 mm can be evaluated using the same experimental setup based on specular reflection [10]. This work aims to show that the same setup is suitable as a corneal topographer.

In Section 2, the proposed method is briefly described; then, the design parameters of the null-screen are shown and the experimental setup is fully explained in Sections 3 and 4, respectively. Later, in Section 5, experimental results of the corneal surface reconstruction of a human volunteer are presented. Finally, the conclusions are presented in Section 6.

2. Proposed Setup and Method

As mentioned before, we use four identical null-screens type Hartmann into a quadrangular acrylic prism. The corneal surface of a human volunteer is placed just in front of the quadrangular prism, as shown in Fig. 1.

The essential idea consists of designing an array of null screens with a set of spots in such a way that the image reflected by the corneal surface gives a perfectly ordered arrangement type Hartmann, if the test surface is perfect. Null-screen testing has the advantage that this technique does not need any additional optical element with a specific design to correct the aberrations of the system under test and the spots of the screen can be easily computed [8].

3. Parameters to the Design of Flat Null-Screen

To determine the points on the null-screen belonging to a square array of spots on the CCD sensor, we performed a reverse exact ray-tracing calculation, similarly as they have been obtained in previous work [6]; we use the same expression to get z_3, the calculation only differs in the use of four flat null-screens (parallel to the x and y axes), instead of three. In null-screen method is used to find the coordinates of the points on screen $P_3=(x_3, y_3, z_3)$ that yield a perfect square array on the CCD; then, we start at the CCD plane. The variables involved in the design of the flat null-screen are shown in Fig. 2; in addition, a calibration sphere is placed as a corneal simulator.

The point $P_1=(x_1, y_1,-a-b)$ and the point $P_2=(x_2, y_2, z_2)$ are the cartesian coordinates on the CCD sensor and in the optical surface respectively, *a* and *b* are distances obtained by the *Gauss thin lens equation* and by the *magnification of the lens used*, these equations can be seen in detail in ref. [6]. The parameters *a* and *b* can be recalculated using the proposal developed by Aguirre-Aguirre et al, ref. [11]. The numerical values of the parameters used in this case are shown in Table 1.

Table 1. Parameters used for calculating the coordinates of flat null-screens.

Element	Description	Symbol	Value (*mm*)
CCD sensor	Thorlabs Model (**DCU223M**)	*d*	3.6 active area
Camera lens	Thorlabs Model (**MVL25M23**)	*f*	25
Parameter	Distance between CCD sensor and camera lens	*a*	29.61
Parameter	Distance between vertex surface and camera lens	*b*	266.07

4. Experimental Setup

To build the practical system, we used four identical flat screens, their dimensions are: 260 mm (height) × 180 mm (width) per side correspondingly. The screens were put side by side to form a quadrangular prism. To classify each null-screen-colored marking (R, G, B and Y) have been designed, which, help to distinguish each side of null-screens inserted in the rectangular prism. As a proof of this principle, Fig. 3. (a) shows a low-cost experimental setup based on specular reflection. The image of the light reflected by the human cornea is nearly seen as a square array of dots captured by the CCD sensor, as is shown in Fig. 3. (b). The reflection of the adaptable Hartmann pattern provides data allowing accurate reconstruction of the surface profile of the corneal surface.

It can be seen that at some points of the null-screen, we paint strategic marks of color following the next basic rules: Six colored spots are set along the *x*-axis, while six spots are positioned along the *y*-axis. For example in Fig. 3 (a), we can see six red spots in the experimental setup along the *z*-axis, just to be redundant, in the orthogonal side, it is easy to see six green spots along the *z*-axis. This set of colored spots allows relating "*x*" and "*y*" directions on the screens even if one-or two-colored spots are missing. Due to the sticking of null-screens on edges of the square prism some spots on the image are missing; that, complicates the final correspondence between centroids and coordinates of the null-screens. For this, the same reference color marks designed in null-screens (R, G, B and Y) helps to the correspondence during the quantitative evaluation of optical surfaces [Fig. 3. (b)].

4.1 Zonal Integration

Having the information of the positions of the centroids and the knowledge coordinate to the flat null-screens, normal components to the surface are calculated, according to procedures proposed in [5-6], [9-11]. To evaluate the normals ***N***, to the test surface, we perform a three-dimensional ray trace procedure, which consists of finding directions of the rays that join actual positions, P_1, of centroids of the experimental image, and the

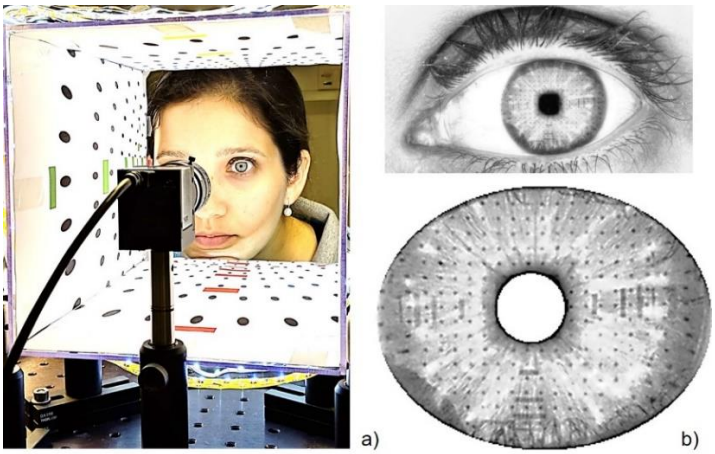

Fig. 3. (a) Experimental setup of corneal Topographer, (b) Detail of the reflected pattern.

corresponding coordinates *P3* of null-screen. According to reflection law, normal ***N*** to the test surface can be evaluated as.

$$N = \frac{R - I}{|R - I|}. \tag{1}$$

Where ***I*** and ***R*** are the directions of the incident and reflected rays on the surface, respectively. The direction of the reflected ray ***R*** is known because after reflection on the test surface it passes through the center of the lens stop at ***P*** and arrives at the CCD image plane at $\boldsymbol{P_1}$, so that, we have two points along this ray, which are enough to know its direction (see Fig. 2). In contrast, for incident ray ***I***, we know only the point $\boldsymbol{P_3}$ at null-screen, so, we need to have an approximate second point to obtain the direction of the incident ray; this is done by intersecting the reflected ray with a *reference surface*.

The shape of the surface is obtained by using the equation originally proposed by Díaz-Uribe [12] and first used in [8].

$$z - z_1 = \int_{\wp(x_1, y_1)}^{(x,y)} \left[\frac{N_x}{N_z} dx + \frac{N_y}{N_z} dy \right]. \tag{2}$$

Where; $\boldsymbol{N}x$, $\boldsymbol{N}y$, and $\boldsymbol{N}_z$ are the cartesian components of the normal vector, C is the integration path, z_1 is the initial point in the integration path. Eq. (2) is exact, evaluating normals and performing the numerical integration, however, are approximate, so they introduce some errors that must be reduced. Thus, the errors involved during the determination of the normals are minimal if the reference surface differs only slightly from the test surface. The numerical evaluation of Eq. (3) can be performed by zonal or modal procedures; a simple zonal evaluation of the integral is the trapezoidal rule for nonequally spaced data [12-13], as

Table 2. Principal Coefficients of the Zernike Standard Polynomial.

Zernike Standard Polynomial	Coefficient (**μm**)	Zernike Standard Polynomial	Coefficient (**μm**)
Vertical Astigmatism (Z_6)	14.0357	Vertical Coma (Z_7)	5.4472
Primary Spherical (Z_{11})	7.4266	Horizontal Coma (Z_8)	-3.2004

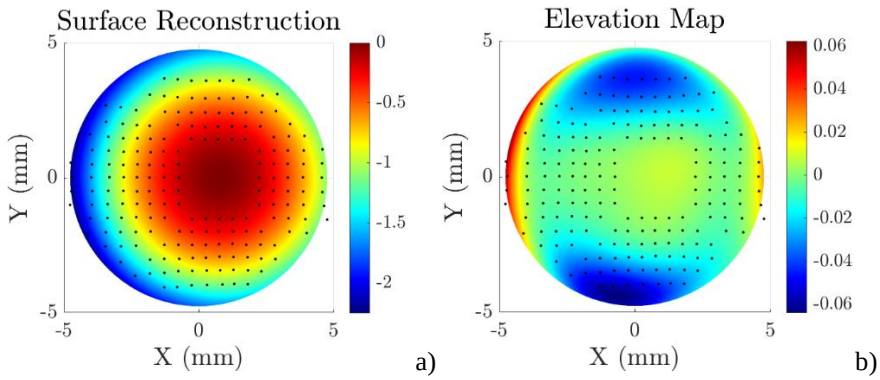

Fig. 4. Results: a) Shape surface reconstruction obtained by Zonal integration method, b) Elevation Color Map represented by Zernike standard Polynomial, (in mm units).

$$z_M = -\sum_{i=1}^{M-1}\left\{\left(\frac{N_{x_i}}{N_{z_i}}+\frac{N_{x_{i+1}}}{N_{z_{i+1}}}\right)\left(\frac{x_{i+1}-x_i}{2}\right)+\left(\frac{N_{y_i}}{N_{z_i}}+\frac{N_{y_{i+1}}}{N_{z_{i+1}}}\right)\left(\frac{y_{i+1}-y_i}{2}\right)+z_0\right\}. \quad (3)$$

Where M is the number of points along some integration path.
Consequently, the integration obtained with Eq. (3) and different paths covering all the centroids, the spatial position of every incidence point on the surface is obtained, and the shape surface equation is calculated as described in Refs. [5, 6].

5. Experimental Results

Corneal surface reconstruction obtained by the zonal integration method is shown in Fig 4(a). In addition, we obtained the elevation map (Fig. 4(b)) by taking the differences between the best spherical model and the data obtained by zonal integration. The differences were fitted into a Zernike standard polynomial with 37 terms [14].

In this first evaluation, we found that the radius of curvature of the best fitted sphere was $r_c = 7.84\ mm$. Analyzing the elevation color map, the peak-valley (P–V) value in sagitta differences is $\delta z_{p-v} = 120\mu m$, while the *RMS* value is $\delta z_{rms} = 18\ \mu m$. Table 2 lists the dominating Zernike components from the best fitted sphere. Results show that the dominated component is vertical astigmatism (Z_6).

6. Conclusions

In this paper, a quadrangular prism configuration based on null-screens has been proposed. This aimed at the measurement of corneal topography, so experimental results obtained for a human corneal have been presented. The radius of curvature becomes closer to the real value; on the other hand, the RMS difference in sagitta which represent the elevation color map is within the range of commercial topographers, with $\delta z_{RMS} = 18\ mm$. Finally, we notice that the dominating components of the Zernike standard polynomials are Astigmatism (Z_6, Z_8), Primary Spherical (Z_{11}), Vertical Coma (Z_7) and Horizontal Coma (Z_8). The results obtained do not represent a fundamental limit; they can be improved with better alignment of the quadrangular setup of the surface or by improving the numerical routines.

Acknowledgment. The corresponding author thanks to the projects DGAPA-PAPIIT: **TA101620**, **IT100321** and **IT102520**. Dulce Gonzalez-Utrera acknowledges to postdoctoral research grant from CONACyT México.

References

1. Rand, R., Applegate, R.A., Howland, H.C.: A mathematical model of Placido disk keratometer and its implication for recovery of corneal topography. In: Vision Science and Its Applications. OSA Technical Digest Series, 1, pp. 46–49, (1997)
2. Schwiegerling, J., Miller, J.M.: A videokeratoscope using a distorted checkerboard target. In: Vision Science and Its Applications (OSA Annual Meeting), (1998)
3. Klein, S.A.: Axial curvature and the skew ray error in corneal topography. In: Vision Science and Its Applications, 74, pp. 931–994, (1997)
4. Klein, S.A.: Corneal topography reconstruction algorithm that avoids the skew ray ambiguity and the skew error. In: Vision Science and Its Applications, 74, pp. 945–962, (1997)
5. Campos-García, M., Cossio-Guerrero, C., Moreno-Oliva, V.I., Huerta-Carranza, O.: Surface shape evaluation with a corneal topographer based on a conical null-screen with a novel radial point distribution. Applied Optics, 54, pp. 5411–5419, (2015)
6. Rodríguez-Rodríguez, M.I., Jaramillo-Nuñez, A., Díaz-Uribe, R.: Dynamic point shifting with null screen using three LCDs as targets for corneal topography. Applied Optics, 54, pp. 6698–6710, (2015)
7. Mejía-Barbosa, Y., Malacara-Hernández, D.: Object surface for applying a modified Hartmann test to measure corneal topography. Applied Optics, 40, pp. 5778–5786, (2001)
8. Díaz-Uribe, R., Campos-García, M.: Null-screen testing of fast convex aspheric surfaces. Applied Optics, 39, pp. 2670–2677, (2000)
9. Gonzalez Utrera, D., Aguirre-Aguirre, D., Rodríguez-Rodríguez, M.I., Díaz-Uribe, R.: Null-screen testing of the complementary freeform surfaces of an adjustable focus lens. Optics Express, 29(14), pp. 21698–21710, (2021)
10. Rodríguez-Rodríguez, M.I., Carmichael Martins, A., Vohnsen, B., Díaz-Uribe, R., Malacara-Hernández, D.: Corneal topographer using a Hartmann patterned. In: Proceedings of RIAO, (2019)
11. Aguirre-Aguirre, D., Díaz-Uribe, R., Campos-García, M., Villalobos-Mendoza, B., Izazaga-Pérez, R., Huerta-Carranza, O.: Fast conical surfaces evaluation with null-screen and randomized algorithms. Applied Optics, 56, pp. 1370–1382, (2017)

12. Díaz-Uribe, R.: Medium precision null screen testing of off-axis parabolic mirrors for segmented primary telescope optics; the case of the Large Millimetric Telescope. Applied Optics, 39, pp. 2790–2804, (2000)
13. Noll, R.J.: Zernike polynomials and atmospheric turbulence. Journal of the Optical Society of America, 66, pp. 207–211, (1976)